# We are IntechOpen, the world's leading publisher of Open Access books Built by scientists, for scientists

**6,900**
Open access books available

**186,000**
International authors and editors

**200M**
Downloads

**154**
Countries delivered to

Our authors are among the

**TOP 1%**
most cited scientists

**12.2%**
Contributors from top 500 universities

CLARIVATE ANALYTICS
**BOOK CITATION INDEX**
INDEXED

**WEB OF SCIENCE**™

Selection of our books indexed in the Book Citation Index
in Web of Science™ Core Collection (BKCI)

## Interested in publishing with us?
Contact book.department@intechopen.com

# Optimized Method for Real Time Nonlinear Control

Younes Rafic[1], Omran Rabih[1] and Rachid Outbib[2]
*[1]Lebanese University, Faculty of Engineering, Beirut*
*[2]LSIS, Aix-Marseilles University, Marseille*
*[1]Lebanon*
*[2]France*

## 1. Introduction

In this chapter, we discuss the problem of systems control. This problem represents the most important challenge for control engineers. It has attracted the interest of several authors and different approaches have been proposed and tested. These approaches can all be divided into two categories; Linear and Nonlinear approaches. In linear approaches, the analysis and the synthesis are simple however the results are limited to a specified range of operation. In nonlinear approaches, the results are valid in a large domain however the analysis is very complex. We should also note that some works on feedback control are dedicated to the feedback linearization in order to make the models, when it is possible, linear by using a preliminary feedback.

The most important and well-known methodologies about control analysis and feedback control are the following: PID approach, Describing function method, adaptive control, robust control, Lyapunov stability, singular perturbation method, Popov criterion, center manifold theorem and passivity analysis.

The first step in the controller design procedure is the construction of a *truth model* which describes the dynamics of the process to be controlled. The truth model is a *simulation model* that includes the basic characteristics of the process but it is too complicated to be used in the control design. Thus, we need to develop a simplified model to be used instead. Such a model is defined by Friedland (Friedland, 1991) as the *design model*. The design model should capture the essential features of the process.

In order to describe the behavior of the process, a continuous dynamic system constituted by a finite set of ordinary differential equations of the following form is used:

$$\dot{x} = F[t, x(t), u(t)] \qquad x(t_0) = x_0$$
$$y(t) = H[t, x(t), u(t)] \tag{1}$$

where the state $x \in \mathbf{R}^n$, the input $u \in \mathbf{R}^m$, the output $y \in \mathbf{R}^p$, and $F$ and $H$ are vector-valued functions with $F : \mathbf{R} \times \mathbf{R}^n \times \mathbf{R}^m \to \mathbf{R}^n$ and $H : \mathbf{R} \times \mathbf{R}^n \times \mathbf{R}^m \to \mathbf{R}^p$.

A second kind of used model is the discrete dynamic system defined by a finite set of difference equations:

$$x(k+1) = F[k, x(k), u(k)] \quad x(k_0) = x_0$$
$$y(k) = H[k, x(k), u(k)]$$
$$(2)$$

where $x(k) = x(kh)$, $u(k) = u(kh)$, $h$ is the sampling time interval, and $k \geq 0$ is an integer.

The objective of this chapter is to propose a new strategy for control design using optimization method which is suitable for real time applications. This new methodology is based on neural network which is the classical approach to treat practical results using experimental tests. In order to illustrate this methodology and its applications, we will present an example of the intake air manifold control in a Diesel internal combustion engine.

The chapter is divided as follows: In the second section a short overview of classical control methods is presented. In the third section a new methodology for control is proposed. In the fourth section, we present the application of the new control methodology to the Diesel engine. And finally, we end this chapter with our conclusions and remarks.

## 2. Overview of classical control methods

A main goal of the feedback control system is to guarantee the stability of the closed-loop behavior. For linear systems, this can be obtained by adapting the control parameters of the transfer function which describes the system in a way so that the real parts of its poles have negative values. Otherwise, Nonlinear control systems use specific theories to ensure the system stability and that is regardless the inner dynamic of the system. The possibility to realize different specifications varies according to the model considered and the control strategy chosen. Hereafter we present a summary of some techniques that can be used:

### 2.1 Theory of Lyapunov

Lyapunov theory is usually used to determine the stability properties at an equilibrium point without the need to resolve the state equations of the nonlinear system. Let us consider the autonomous non-linear system

$$\dot{x} = F(x) \tag{3}$$

where $x \in R^n$ is the state variable of the system and $F$ is a smooth vector field. Assume that there is a function $V$ defined as follows:

$V : R^n \rightarrow R_+$ so that $V(x) = 0 \Leftrightarrow x = 0$ and $\lim_{x \to \infty} V(x) = +\infty$ If the derivative of $V$ along the trajectories of (3) is so that :

$$\dot{V} = \prec \nabla V(x), F(x) \succ < 0 \quad \text{for all} \quad x \neq 0 \tag{4}$$

where $\nabla$ designates the gradient and $\prec ., . \succ$ denotes the scalar product, than the system (3) is globally asymptotically stable. This is the Theorem of Lyapunov (Hahn, 1967). This approach has been improved in the principle of Krosoviskii-LaSalle (Hahn, 1967). In fact, it is shown that the condition given by (4) can be relaxed to

$$\dot{V} = \prec \nabla V(x), F(x) \succ \leq 0 \text{ for all } x \tag{5}$$

under the hypothesis that the more invariant set, by (3), included in

$$\Omega = \left\{ x \in R^n / \dot{V} = 0 \right\} \tag{6}$$

is reduced to the origin.

These two theorems are the base of a large number of results on analysis of stability for nonlinear systems. In fact, the theory of Lyapunov- Krosoviskii-LaSalle is fundamental and is the base of this analysis. In the literature, this theory can have various versions according to the nature of the problem, for instance, for discrete models, stochastic systems or partial differential equations.

In addition to the methodologies developed before, the theory is used to describe the control problems. The use of this theory is illustrated by the following result of feedback stabilization.

Let us consider the following controlled system

$$\dot{x} = F(x) + u \cdot G(x) \tag{7}$$

where $x \in R^n$ is the state, $u \in R$ is the control variable, $F$ and $G$ are smooth vector fields. Assume there is $V$ a Lyapunov function so that

$$\dot{V} = \prec \nabla V(x), F(x) \succ \leq 0 \tag{8}$$

Under some hypothesis is proved (Outbib, 1999) that the closed-loop system defined from (7) with

$$u = - \prec \nabla V(x), G(x) \succ \tag{9}$$

is globally asymptotically stable at the origin. A simple example to illustrate this result is the scalar system

$$\dot{x} = u \tag{10}$$

Clearly, the system verifies the hypothesis with $V(x) = 1/2 \cdot x^2$ and the stabilizing control $u = -x$ can be deduced. This approach has been applied to practical process (Outbib, 2000; Dreyfus, 1962)

## 2.2 Adaptive control

The adaptive control is mainly used in cases where the control law must be continuously adapted due to the varying nature of the system parameters or its initial uncertainties.

Let us consider the following non linear system

$$\dot{x} = F(x, \theta) \tag{11}$$

Where $x$ denotes the state variable of the system and $\theta$ designates a parameter. The adaptive control is used in the situation where the parameter $\theta$ is not known or can change. For example, let us consider the scalar classical system:

$$\dot{x} = \theta \cdot x^2 + u \tag{12}$$

If $\theta$ is known the system (12) can be globally asymptotically stable using a control law of the form $u = -\theta \cdot x^2 - k(x)$, where $k$ is any smooth scalar function defined as follow: $k(x)x > 0$ for $x \neq 0$.

The certainty-equivalent controller is defined by

$$\begin{cases} u = -\hat{\theta} \cdot x^2 - k(x) \\ \dot{\hat{\theta}} = w \end{cases} \tag{13}$$

where $w$ is the update law.
Let $V$ be the Lyapunov function defined by:

$$V(x,\theta) = \frac{1}{2} \cdot x^2 + \frac{\alpha}{2} \cdot \left(\hat{\theta} - \theta\right)^2 \tag{14}$$

with $\alpha > 0$. The derivative of the closed-loop system defined from (12) and (13):

$$\begin{cases} u = -(\theta - \hat{\theta}) \cdot x^2 - k(x) \\ \dot{\hat{\theta}} = w \end{cases} \tag{15}$$

is given by

$$\dot{V}(x,\theta) = -x \cdot k(x) - \left(\hat{\theta} - \theta\right) \cdot x^3 + \alpha \cdot \left(\hat{\theta} - \theta\right) \cdot w \tag{16}$$

Now, if we let $w = (1/\alpha) \cdot x^3$, we get

$$\dot{V}(x,\theta) = -x \cdot k(x) \leq 0 \; for \; all \; x \tag{17}$$

This implies that $(x, \hat{\theta})$ is bounded and $x$ converges to zero and ensures that the system (12) can be stabilized at the origin.

## 2.3 Sliding mode control

The Russian school developed the methodology of sliding mode control in the 1950s. Since this time, the technique has been improved by several authors (Slotine, 1984; Utkin, 1992; Sira-Ramirez, 1987; Bartoloni, 1989; Outbib & Zasadzinski, 2009). This approach is applicable to various domains, including aerospace, robotics, chemical processes, etc.

The sliding mode control is a variable structure control method. Its principle is to force the system to reach and to stay confined over specific surfaces where the stability can be ensured, and that is based on discontinuous control signal.

In order to illustrate the approach based on variable structure control, we now present a simple example. Let us consider the scalar system defined by:

$$\ddot{x} = u \tag{18}$$

Our goal is to propose a control law of the form $u = u(x)$ so that $\lim_{x \to +\infty} x(t) = \lim_{x \to +\infty} \dot{x}(t) = 0$. Clearly, the system (18) can be globally asymptotically stable using a control law of the form $u = f(x, \dot{x})$. In fact, one can use for instance $u = -x - \dot{x}$.

Now a simple analysis can show that there is no linear control law, of the form $u = ax$, which makes the system globally asymptotically stable at the origin. But, if we consider a state feedback that commutes between two linear laws of the form:

$$u = \begin{cases} a_1 \cdot x & if \ \ x \cdot \dot{x} > 0 \\ a_2 \cdot x & if \ \ x \cdot \dot{x} < 0 \end{cases} \tag{19}$$

than the system can be globally asymptotically stable using appropriate values for $a_1$ and $a_2$.

## 2.4 Optimal control

The objective of the optimal control method is to search for the best dynamic course which is capable of transporting the system from an initial state to a final desired state at minimum cost. An example of its various applications can be found in the satellite control. More precisely, the optimal control technique can be defined as follows:

Let us consider the following system:

$$\dot{x} = F(t, x(t), u(t)) \tag{20}$$

where $x \in \mathbf{R}^n$ designates the state variable and $u \in \mathbf{R}^m$ is the control variable. $f : R \times R^n \times R^m \to R^n$ is a smooth vector-valued function .The optimal control is to find a suitable dynamic control $u(t)$ which allows the system to follow an optimal trajectory $x(t)$ that minimizes the cost function :

$$J = \int_{t0}^{t1} H(t, x(t), u(t)) \tag{21}$$

Several approaches have been used to resolve this problem. Among these approaches we can cite the variational calculus (Dreyfus, 1962), the maximum principle of Pontryagin (Pontryagin, 1962) or the procedure of dynamic programming method of Bellman (Bellman, 1957).

Let us consider a simple example such as the hanging pendulum. The equation describing the movement of the pendulum angular position under an applied torque $\alpha$ is given by:

$$\begin{cases} \ddot{\theta}(t) + \lambda \cdot \dot{\theta}(t) + \omega^2 \cdot \theta(t) = \alpha(t) \\ \quad \theta(0) = \theta_1 \quad \dot{\theta}(0) = \theta_2 \end{cases} \tag{22}$$

where $\theta$ designates the angular position at time $t$. Let $x$ be the system state variable $x = \left[ \theta(t), \dot{\theta}(t) \right]$, we can write :

$$\dot{x}(t) = \begin{pmatrix} x_2 \\ -\lambda \cdot x_2 - \omega^2 \cdot x_1 + \alpha \end{pmatrix} = f(x, \alpha) \tag{23}$$

Therefore the optimal control goal can be to minimize the time interval $\tau$, in order to reach the state values $x(\tau) = 0$.

### 2.5 Robust control

The objective of robust control is to find a control law in such a way that the response of the system and the error signals are maintained to desired values despite the effects of uncertainties on the system. The uncertainties sources can be any disturbance signals, the measurement noise or the modeling errors due to none considered nonlinearities and time-varying parameters.

The theory of robust control began in the 1970s and 1980s (Doyle, 1979; Zames, 1981) with some aircraft applications. Actually, its applications concern different domains (aerospace, economics, ...).

## 3. New algorithm for Optimized Nonlinear Control (ONC)

The objective of this methodology is to propose a system optimized dynamic control which can be used in real time control applications. The proposed methodology (Omran, 2008b) can be divided into five steps: 1) Modeling process, 2) Model validation, 3) Dynamic optimization process, 4) Creation of a large database of the optimal control variables using the dynamic optimization process, 5) The neural network controller.

In the next sub-sections, we present the different methodology steps and we explain its application using the example of the Diesel engine system.

### 3.1 Modeling process

The general equations which describe the functioning of a system can be expressed using the following form (Rivals, 1995):

$$\begin{cases} \dot{X} = F(X, I, u, t) \\ Y = g(X, I, u, t) \end{cases} \tag{24}$$

Where $F$ and g are nonlinear functions, $X$ is the system state variables, $I$ is the inputs variables, $u$ is the control variables to be tuned and Y is the output.

### 3.2 Experimental validation

In this phase we used specified experimental data to identify the model parameters used in the modeling process (models of representation: transfer function or neural networks, models of knowledge,…), and than we used dynamic experimental data to test the model responses accuracy and its validation. This step is classic in any modeling process.

### 3.3 Offline dynamic optimization

In this step we present the optimization technique of the control variables over dynamic courses and we define the objective function to be used. The question that we should ask is the following: In response to dynamic inputs I(t) which solicit the system over a certain interval of time [0,T], what is the optimal continuous values of the control parameters u(t) which minimize the cumulative production of the output Y(t). Therefore the objective function to be minimized can be written using the following form:

$$\underset{a_i}{Min}\int_0^T Y(t)\cdot dt = \underset{a_i}{Min}\int_0^T g(X,I,u,t)\cdot dt \tag{25}$$

The optimization problem has the following equalities and inequalities constraints:

Equalities constraints:
$$\frac{dX}{dt} = F(X,I,u,t) \tag{26}$$

Inequalities constraints:
$$\begin{array}{c} X_{\min} < X < X_{\max} \\ u_{\min} < u < u_{\max} \end{array} \tag{27}$$

Because the problem is nonlinear, there is no analytical solution; therefore we must reformulate it into its discretized form as following:

Objective function:
$$\underset{a_i}{Min}\sum_{i=1}^N g_i(X_i,I_i,u_i,t_i) \tag{28}$$

Equality constraints:
$$\frac{dX}{dt} = F(X,I,u,t) \Rightarrow \frac{X_{i+1}-X_i}{\Delta t} = F_i(X_i,I_i,u_i,t_i)$$

$$X_{i+1} - X_i - \Delta t.F(X_i,I_i,u_i,t_i) = 0 \tag{29}$$

Inequality constraints:
$$\begin{array}{c} X_{\min} < X_i < X_{\max} \\ u_{\min} < u_i < u_{\max} \end{array} \tag{30}$$

The inequality constraints are the domain definition of the system's state and control variables; they are the lower and upper physical, mechanical or tolerance limits which assure a good functioning performance of the system and prevent the system damage. In our case, for example, the engine speed and the intake and exhaust pressure and temperature must vary between a lower and upper limit to prevent engine system damage or dysfunction.

### 3.4 Creation of the optimal database

The optimization problem explained previously necessitates a long computation time and therefore it cannot be directly resolved in real time applications, in addition the inputs evolution must be known beforehand which is not true in any real time applications. Consequently we propose to resolve the problem off line for different inputs profiles that

are very rich in information and variety and that cover a large area of possibility of the system's domain and then to regroup the found solutions (inputs profiles and optimal control variables) in a large database which will be exploited in the following step. Therefore in the created database, we will find for every input vector I(t) an output vector u(t) which is the optimal control variables that can be used to respond to the inputs solicitations. In the next section this database will be used to create a dynamic controller based on neural networks.

### 3.5 Online neural network control

Since a score of year, the neural networks are considered as a powerful mathematical tool to perform nonlinear regression. Many engineers used them as a black box model to estimate the system responses and they also used them in various fields of applications including pattern recognition, forms recognition, objects classification, filters and control systems (Rivals, 1995). We distinguish two main types of neural networks: feed-forward or multi-layers networks used for steady state processes and feedback or recurrent networks used for dynamic processes. We recognize to these networks the following fundamental characteristics (Ouladssine, 2004): They are black box models with great capacity for universal, flexible and parsimonious functions approximation.

We are interested in establishing a control technique by training a recurrent neural network using the database created in the forth step of this methodology. The main advantage of this approach is essentially the capacity of developing a nonlinear controller with a small computation time which can be executed in real time applications.

Between the various neural networks architectures found in the literature, the multi-layer perceptrons are the most popular; they are particularly exploited in system modeling, identification and control processes (Zweiri 2006). Many works show that the three layers perceptrons with one hidden layer are universal function approximation (Li, 2005); they are capable to approximate any nonlinear continuous function, defined from a finite multi-dimensions space into another, with an arbitrary fixed precision, while they require the identification of a limited number of parameters comparing to the development of series of fixed functions. In this way, they are parsimonious.

## 4. Application: Optimal air control in diesel engine

Many vehicles developers are especially interested in Diesel internal combustion engines because of their high efficiencies reflecting low fuel consumption. Therefore, electronics and common rail injection systems are largely developed and used in diesel engines along with variable geometry turbocharger and exhaust gas recirculation in order to reduce the pollution and protect the environment and the human health and to optimize the engine performance and fuel consumption. The future engines must respect the more restricted pollution legislations fixed in the European emissions standards (table 1). The particulate matter that are mostly emitted under transient conditions due to air insufficiency are expected to be reduced of a ratio 1:10 at 2010 (Euro 6) and the nitrogen oxides which are caused by a smaller rate of the exhaust gas recirculation due to the insufficiency of fresh air supplied to the engine by the compressor at low engine speed and fuel consumption reduction and engine performance at high speed are also supposed to be reduced to half.

| Heavy duty vehicle | Euro 1 1993 | Euro 2 1996 | Euro 3 2000 | Euro 4 2005 | Euro 5 2008 | Euro 6 2010 |
|---|---|---|---|---|---|---|
| Oxides nitrogen | 9 | 7 | 5 | 3,5 | 2 | 1 |
| Carbon monoxide | 4,5 | 4 | 2,1 | 1,5 | 1,5 | 1,5 |
| Hydro-carbons | 1,23 | 1,1 | 0,66 | 0,46 | 0,46 | 0,46 |
| Particulate Matter | 0,4 | 0,15 | 0,1 | 0,02 | 0,02 | 0,002 |

Table 1. European standard of heavy duty vehicles in g/KW.h

Actually, modern diesel engines are controlled by look up tables which are the results of a steady state optimization using experiments done on a test bench. Figure 1 shows a static chart of the fresh air flow rate that is used to control the air management system. This chart, as well as the entire look up tables used in the engine control, depends over two entries: the crankshaft angular speed and the fuel mass flow rate (Arnold, 2007). The schematic description of an open and closed loop control are shown in fig. 2 and 3. The inputs are the pedal's position $X_p$ and the engine angular speed w. The outputs are the actuators of the turbine variable geometry $GV$ and the opening position of the exhaust gas recirculation EGR. The indication *ref* designates a reference value and the indication *corr* is its corrected value. $P$ and $m'_C$ are respectively the predicted or measured intake pressure and the air mass flow rate entering the intake manifold.
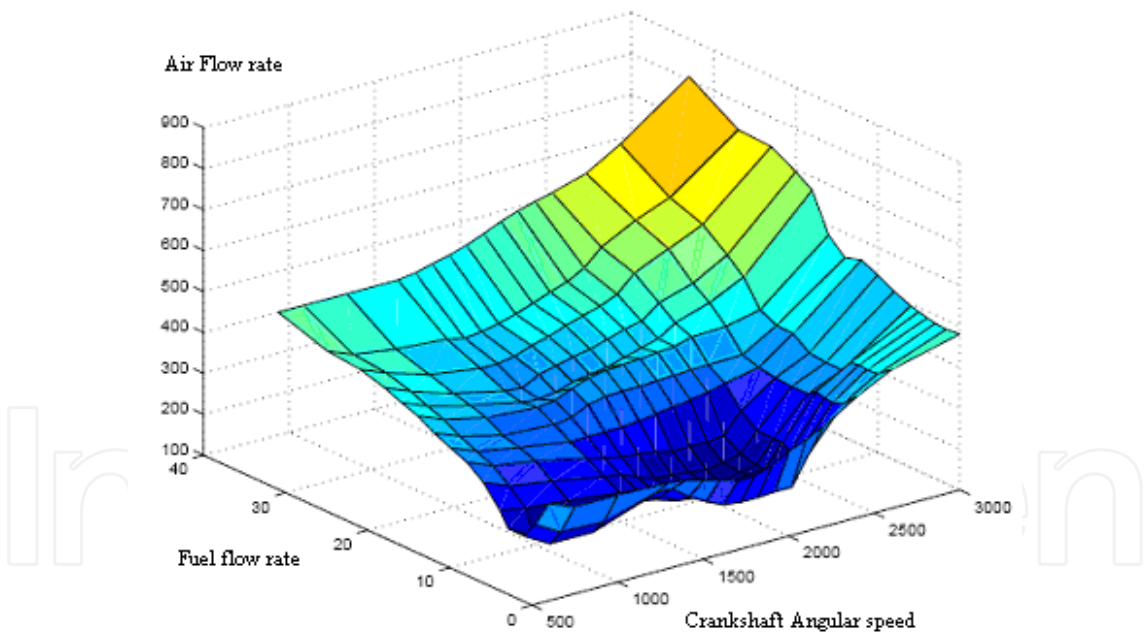


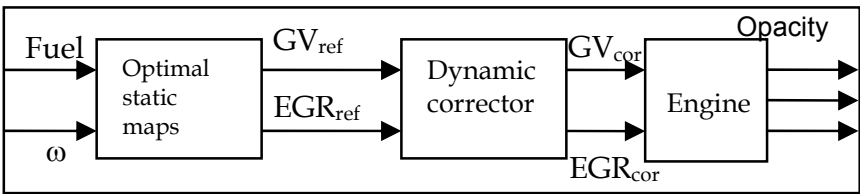Fig. 1. Static chart of the fresh air flow rate used in the engine control schemes.
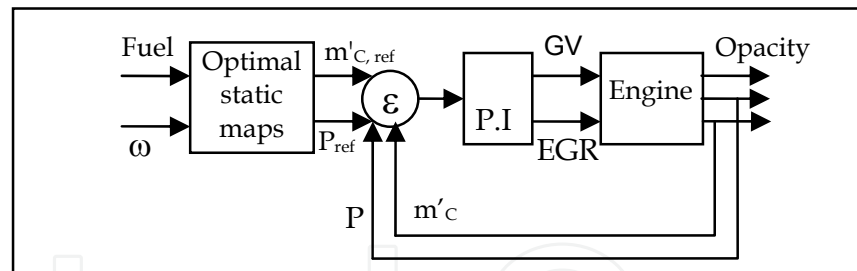


Fig. 2. Open loop control

Fig. 3. Closed loop control

In the open loop control, the classic control of a diesel engine (Hafner, 2000) is done according to the diagram in fig. 2, the optimal values of the actuators are updated by memorized static maps. Then a predictive corrector (Hafner, 2001) is generally used in order to compensate the engine dynamic effects.

In the closed loop control (fig. 3), the engine is controlled by error signals which are the difference between the predicted or measured air mass flow rate and the intake pressure, and their reference values. The controller uses memorized maps as reference, based on engine steady state optimization (Hafner, 2001; Bai, 2002). The influence of the dynamic behavior is integrated by several types of controller (PI, robust control with variable parameters, …) (Jung, 2003).

Our work proposes practical solutions to overcome and outperform the control insufficiency using static maps. The advantage of this approach is to be able to propose dynamic maps capable of predicting, "on line", the in-air cylinders filling. Therefore the optimal static maps in fig. 1 and 2 can be replaced by optimal dynamic ones.

We suggest a mathematical optimization process based on the mean value engine model to minimize the total pollutants production and emissions over dynamic courses without deteriorating the engine performance. We used the opacity as a pollution criterion, this choice was strictly limited due to the available data, but the process is universal and it can be applied individually to each pollutant which has physical model or to the all assembled together.

This optimization's procedure is difficult to be applied directly in "on line" engines' applications, due to the computation difficulties which are time consuming. Consequently, it will be used to build up a large database in order to train a neural model which will be used instead. Neural networks are very efficient in learning the nonlinear relations in complex multi-variables systems; they are accurate, easy to train and suitable for real time applications.

All the simulations results and figures presented in this section were computed using Matlab development environment and toolboxes. The following section is divided to four subsections as follows: I Engine dynamic modeling, II Simulation and validation of the engine's model, III Optimization over dynamic trajectories, IV Creation of Neural network for "on line" controller.

### 4.1 Engine dynamic modeling

Diesel engines can be modeled in two different ways: The models of knowledge quasi-static (Winterbonne, 1984), draining-replenishment (Kao, 1995), semi mixed (Ouenou-Gamo, 2001; Younes, 1993), bond graph (Hassenfolder, 1993), and the models of representation by transfer functions (Younes, 1993), neural networks (Ouladssine, 2004).

Seen our optimization objective, the model of knowledge will be adopted in this work. The semi-mixed model is the simplest analytic approach to be used in an optimization process.

The Diesel engine described here is equipped with a variable geometry turbocharger and water cooled heat exchanger to cool the hot air exiting the compressor, but it doesn't have an exhaust gas recirculation system that is mainly used to reduce the NOx emissions.

Consequently the engine is divided to three main blocks: A. the intake air manifold, B. the engine block, C. the opacity (Omran, 2008a).

### 4.1.1 Intake air manifold

Considering air as an ideal gas, the state equation and the mass conservation principle gives [4]:

$$V_a \frac{dP_a}{dt} = r.T_a.\left(\dot{m}_c - \dot{m}_{a0}\right) \tag{31}$$

$\dot{m}_c$ is the compressor air mass flow rate, $\dot{m}_{a0}$ is the air mass flow rate entering the engine, $P_a$, $V_a$ and $T_a$ are respectively the pressure, the volume and the temperature of the air in the intake manifold and $r$ is the mass constant of the air. $\dot{m}_{a0}$ is given by:

$$\dot{m}_{a0} = \eta_V \cdot \dot{m}_{a0,th} \tag{32}$$

$\dot{m}_{a0,th}$ is the theoretical air mass flow rate capable of filling the entire cylinders' volume at the intake conditions of pressure and temperature:

$$\dot{m}_{a0,th} = \frac{Vcyl.\omega.P_a}{4 \cdot \pi \cdot r \cdot T_a} \tag{33}$$

$V_{cyl}$ is the displacement, $\omega$ is the crankshaft angular speed, and $\eta_v$ is the in-air filling efficiency given by:

$$\eta_v = a_0 + a_1\omega + a_2\omega^2 \tag{34}$$

Where $a_i$ are constants identified from experimental data. The intake temperature $T_a$ is expressed by:

$$T_a = \left(1 - \eta_{ech}\right) \cdot T_c + \eta_{ech} \cdot T_{water} \tag{35}$$

$T_c$ is the temperature of the air at the compressor's exit. $T_{water}$ is the temperature of the cooling water supposed constant. $\eta_{ech}$ is the efficiency of the heat exchanger supposed constant. The temperature $T_c$ is expressed by:

$$T_c = T_0\left(1 + \left(\left(\frac{P_a}{P_0}\right)^{\gamma-1/\gamma} - 1\right)\frac{1}{\eta_c}\right) \tag{36}$$

### 4.1.2 Engine block

The principle of the conservation of energy applied to the crankshaft gives:

$$\frac{d}{dt}\left(\frac{1}{2}J(\theta)\omega^2\right) = \mathrm{P}_e - \mathrm{P}_r \tag{37}$$

$J(\theta)$ is the moment of inertia of the engine, it is a periodic function of the crankshaft angle due to the repeated motion of its pistons and connecting rods, but for simplicity, in this paper, the inertia is considered constant. $\mathrm{P}_e$ is the effective power produced by the combustion process:

$$\mathrm{P}_e = \eta_e \cdot \dot{m}_f \cdot P_{ci} \tag{38}$$

$\dot{m}_f$ is the fuel flow rate, $P_{ci}$ is the lower calorific power of fuel and $\eta_e$ is the effective efficiency of the engine modeled by [5]:

$$\eta_e = \lambda \cdot \begin{pmatrix} c_1 + c_2 \cdot \lambda + c_3 \cdot \lambda^2 + c_4 \cdot \lambda \cdot w + \\ c_5 \cdot \lambda^2 \cdot w + c_6 \cdot \lambda \cdot w^2 + c_7 \cdot \lambda^2 \cdot w^2 \end{pmatrix} \tag{39}$$

$c_i$ are constants, and $\lambda$ is the coefficient of air excess:

$$\lambda = \frac{\dot{m}_{a0}}{\dot{m}_f} \tag{40}$$

$P_r$ is the resistant power:

$$\mathrm{P}_r = C_r \omega \tag{41}$$

Cr is the resistant torque. Fig. 4 represents a comparison between the effective efficiency model and the experimental data measured on a test bench. The model results are in good agreement with experimental data.
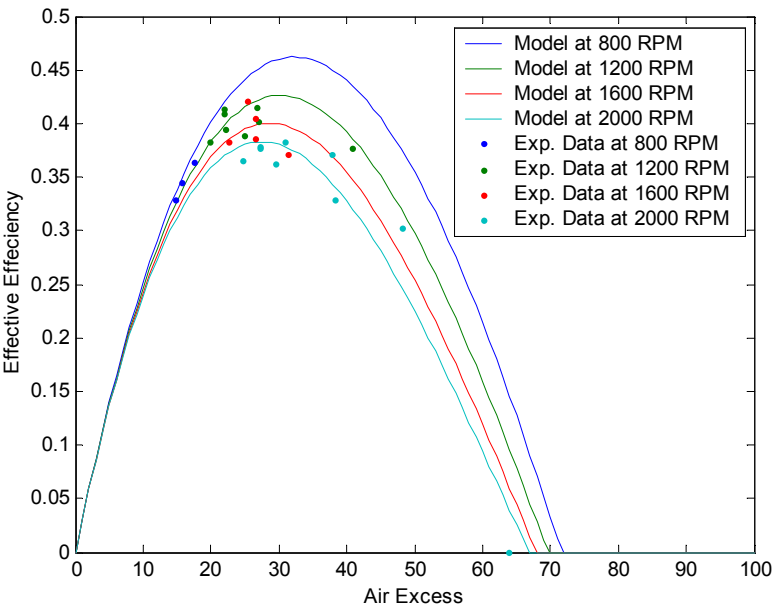


Fig. 4. Comparison between the effective efficiency model results and the experimental data at different crankshaft angular speed.

### 4.1.3 Diesel emissions model

The pollutants that characterize the Diesel engines are mainly the oxides of nitrogen and the particulate matters. In our work, we are especially interested in the emitted quality of smokes which is expressed by the measure of opacity (Fig. 5) (Ouenou-Gamo, 2001):

$$Opacity = m_1 \cdot w^{m_2} \cdot \dot{m}_a^{m_3 \cdot w + m_4} \cdot \dot{m}_f^{m_5 \cdot w + m_6} \tag{42}$$
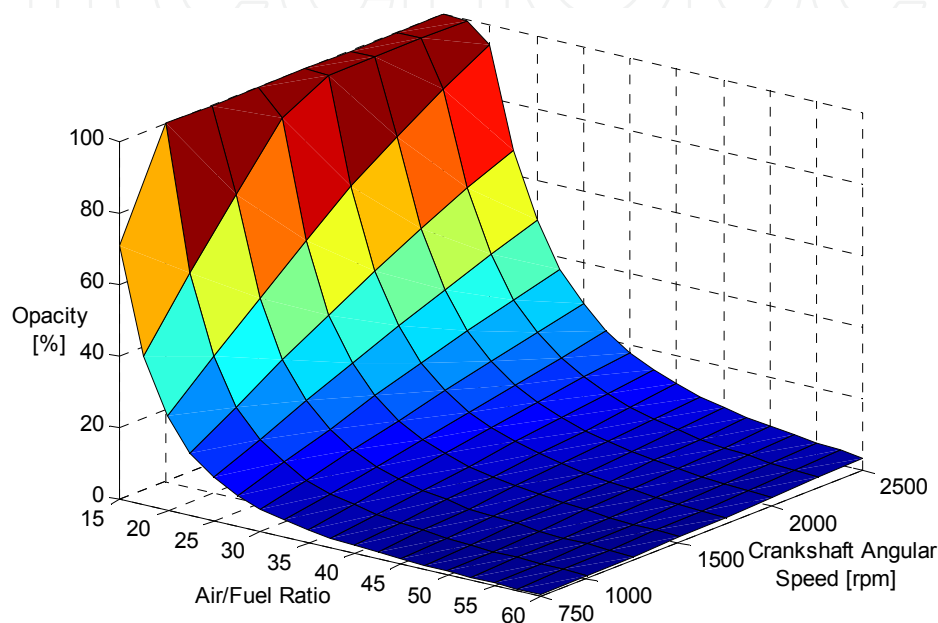
$m_i$ are constants identified from the experimental data measured over a test bench.



Fig. 5. Graphical representation of the opacity computed using (32) and a constant fuel flow rate equal to 6 g/s.

### 4.1.4 System complete model

Reassembling the different blocks' equations leads to a complete model describing the functioning and performance of a variable geometry turbocharged Diesel engine. The model is characterized by two state's variables ($P_a$, $w$), two inputs ($\dot{m}_f$, $C_r$) and the following two differential equations representing the dynamic processes:

$$\begin{cases} V_a \cdot \dfrac{dP_a}{dt} = r \cdot T_a \cdot \left( \dot{m}_c - \dot{m}_{ao} \right) \\ \dfrac{d}{dt}\left( \dfrac{1}{2} J\omega^2 \right) = \eta_e \cdot \dot{m}_f \cdot P_{ci} - C_r \cdot w \end{cases} \tag{43}$$

### 4.2 Model validation

The test bench, conceived and used for the experimental study, involves: a 6 cylinders turbocharged Diesel engine and a brake controlled by the current of Foucault. Engine's characteristics are reported in table 2.

| Stroke [mm] | 145 |
|---|---|
| Displacement [cm3] | 9839.5 |
| Volumetric ratio | 17/1 |
| Bore [mm] | 120 |
| Maximum Power [KW] | 260 |
| at crankshaft angular speed [rpm] | 2400 |
| Maximum torque [daN.m] | 158 |
| at crankshaft angular speed [rpm] | 1200 |
| Relative pressure of overfeeding [bar] | 2 |

Table 2. Engine Characteristics

Different systems are used to collect and analyze the experimental data in transient phase and in real time functioning: - Devices for calculating means and instantaneous measures, - a HC analyzer by flame ionization, - a Bosch smoke detector and - an acquisition device for signal sampling. The use of these devices improves significantly the quality of the static measures by integration over a high number of points.

Fig. 6 and 7 show a comparison between two simulations results of the engine complete model and the experimental data. The inputs of the model are the fuel mass flow rate and the resistant torque profiles. The output variables are: the pressure of the intake manifold $P_a$ the crankshaft angular speed $\omega$ and the opacity characterizing the engine pollution. The differential equations described in section 4.1.4 are computed simultaneously using the Runge-Kutta method. The simulations are in good agreement with the experimental data.
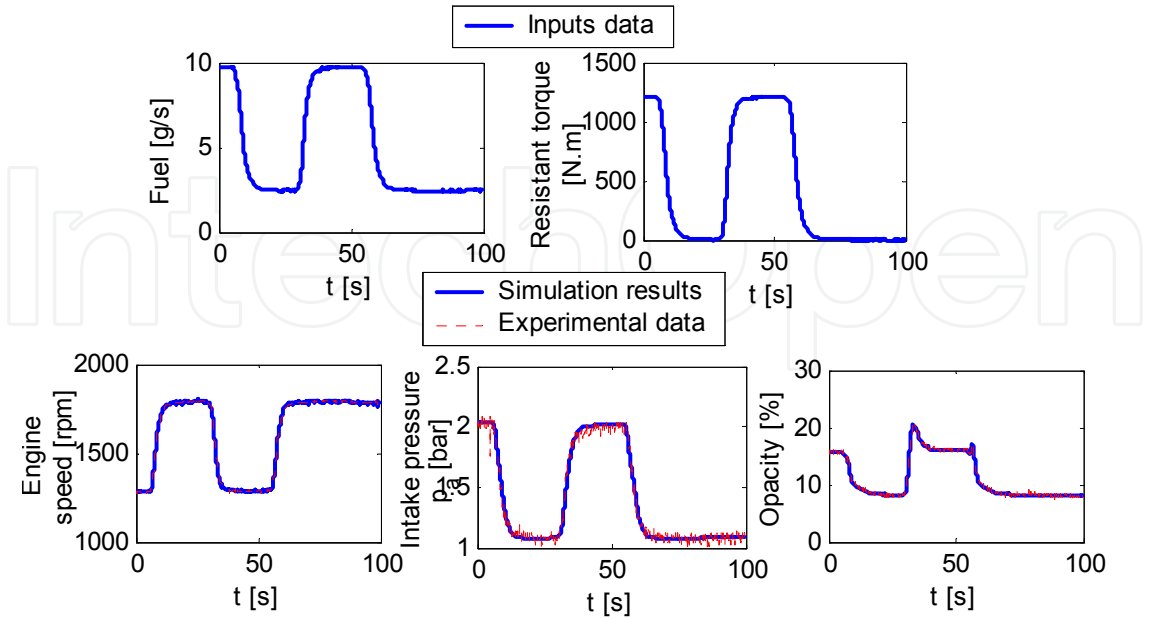


Fig. 6. Simulation 1: Comparison between the complete engine model and the experimental data measured on the test bench.
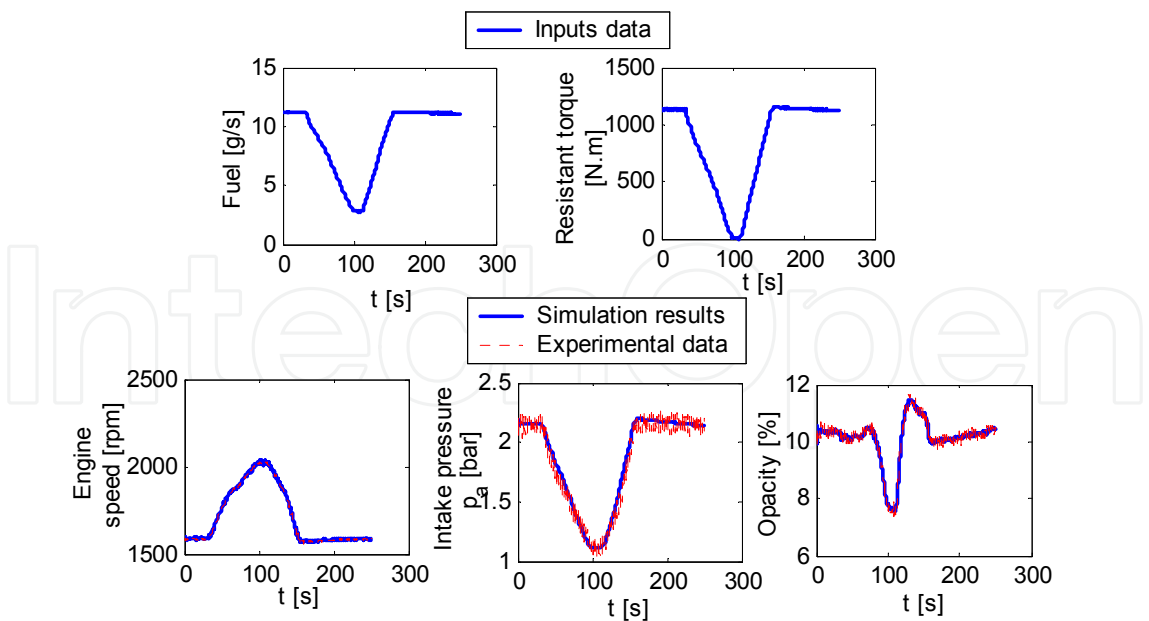
Fig. 7. Simulation 2: Comparison between the complete engine model and the experimental data measured on the test bench.

## 4.3 Optimization process

### 4.3.1 Problem description

When conceiving an engine, engines developers have always to confront and solve the contradictory tasks of producing maximum power (or minimum fuel consumption) while respecting several pollution's constraints (European emissions standard). We are only interesting in reducing the pollutants emissions at the engine level, by applying the optimal "in-air cylinders filling". Consequently, the problem can now be defined; it consists in the following objective multi-criteria function:

$$\begin{cases} \text{Maximize "Power"} \\ \text{Minimize "Pollutants"} \end{cases} \tag{44}$$

This multi-objective optimization problem can be replaced by a single, non dimensional, mathematical function regrouping the two previous criteria:

$$f = -\int \frac{P}{P_{max}} \cdot dt + \sum_i \left\{ \int \frac{Poll_i}{Poll_{i,max}} \cdot dt \right\} \tag{45}$$

P is the engine effective power, $Poll_i$ is a type of pollutant, and the indication *max* characterizes the maximum value that a variable can reach. The integral represents the heap of the pollutants and power over a given dynamic trajectory. This trajectory can be, as an example, a part of the New European Driving Cycle (NEDC).

In this chapter we will only use the opacity as an indication of pollution seen the simplicity of the model and the priority given to the presentation of the method, but we should note that the optimization process is universal and it can involve as many pollution's criteria as we want. The function "objective" becomes:

$$f = -\int \frac{\mathrm{P}}{\mathrm{P}_{max}} \cdot dt + \int \frac{Op}{Op_{max}} \cdot dt \qquad (46)$$

### 4.3.2 Formulation of the problem

The problem consists therefore in minimizing the following function "objective" over a definite working interval [0, t]:

$$f = \left\{ \begin{array}{l} -\dfrac{P_{ci}}{P_{max}} \cdot \int \eta_e \cdot \dot{m}_f \cdot dt \\[2mm] +\dfrac{m_1}{Op_{max}} \cdot \int w^{m_2} \cdot \dot{m}_a^{m_3 \cdot w + m_4} \cdot \dot{m}_f^{m_5 \cdot w + m_6} \cdot dt \end{array} \right\} \qquad (47)$$

Under the equalities constraints representing the differential equations of the engine block and the intake manifold:

$$\left\{ \begin{array}{l} V_a \cdot \dfrac{dP_a}{dt} = r \cdot T_a \cdot \left( \dot{m}_c - \dot{m}_{ao} \right) \\[3mm] \dfrac{d}{dt}\left( \dfrac{1}{2}J\omega^2 \right) = \eta_e \cdot \dot{m}_f \cdot P_{ci} - C_r \cdot w \end{array} \right. \qquad (48)$$

And the inequalities constraints derived from the physical and mechanical limits of the air excess ratio, the intake pressure and the crankshaft angular speed:

$$\left\{ \begin{array}{l} 15 \le \lambda \le 80 \\ 9.5.10^4 \le P_a \le 30.10^4 \quad [Pa] \\ 83 \le \omega \le 230 \quad [rd/s] \end{array} \right. \qquad (49)$$

$\lambda$ is given by:

$$\lambda = \frac{\left(a_0 + a_1\omega + a_2\omega^2\right) \cdot Ncyl.Vcyl.\omega.P_a}{4 \cdot \pi \cdot \dot{m}_f} \qquad (50)$$

The variables of the optimization's problem are $w$, $P_a$ and $m'_c$, and the inputs are $C_r$ and $m'_f$.

We should note that we intentionally eliminate the exhaust and turbo-compressor blocks from the equalities constraints because we are interesting in obtaining the optimal "in-air cylinders filling" $m'_c$ without being limited to any equipments such as the variable geometry turbo-compressor early described. In other words, we can consider that we have replaced the turbo-compressor by a special instrument that can deliver to the intake manifold any value of the air mass flow rate that we choose and at any time. Later, in the conclusion, the devices that can provide these optimal values are briefly discussed. Also we should note that we will use the complete engine model of the existing turbocharged diesel engine as a comparison tool, to prove the validity of our proposed optimal control and the gain in the opacity reduction.

### 4.3.3 Problem discretization

There is no analytic solution to the problem previously formulated; therefore there is a necessity to reformulate it in its discretized form. The integrals in the function "objective" become a simple sum of the functions computed at different instant $t_i$:

$$f = \sum_{i=1}^{N} f_i = f_1 + f_2 + \cdots f_N \tag{51}$$

$N$ is the number of the discretized points, it is the size of the unknown vectors $\vec{\omega}$, $\vec{P}_a$ and $\vec{m}_c$. h is the step of discretization. Using the Taylor development truncated at the first differential order, the equalities constraints become:

$$\begin{cases} P_{a(i+1)} - P_{a(i)} - \dfrac{h}{V_a}\left(r.T_a.\left(\dot{m}_{c(i)} - \dot{m}_{ao(i)}\right)\right) = 0 \\ \omega^2_{(i+1)} - \omega^2_{(i)} - \dfrac{2 \cdot h}{J}\left(P_{e(i)} - P_{r(i)}\right) = 0 \end{cases} \tag{52}$$

And the inequalities constraints:

$$\begin{cases} 15 \le \lambda_{(i)} \le 80 \\ 9.5.10^4 \le P_{a(i)} \le 30.10^4 \quad [Pa] \\ 83 \le \omega_{(i)} \le 230 \quad [rd/s] \end{cases} \tag{53}$$

### 4.3.4 Solution of the optimization problem

The optimization problem under equality and inequality constraints can be described using the following mathematical form:

$$\begin{cases} Min\{f(X)\} \\ X = (x_1, x_2, \ldots x_n) \\ Under\ Constraints \\ h_i(X) = 0 \quad i = 1, \ldots, m \\ g_i(X) \le 0 \quad i = 1, \ldots, p \end{cases} \tag{54}$$

Where $f(X)$ is the objective function, $h(X)$ the equality constraints and $g(X)$ the inequality constraints. The easiest way to resolve this problem is to reduce it to a problem without constraints by creating a global objective function $\Phi(X, h(X), g(X))$ which regroups the original objective function and the equality and inequality constraints (Minoux, 1983).

Therefore we will use a global objective function that regroups: The function "objective", the equalities constraints with Lagrange multipliers, and the inequalities constraints with a penalty function. The final objective function becomes (Minoux, 1983):

$$L(X, \lambda) = f(X) + \sum_{i=1}^{m} \lambda_i * h_i(X) + r.\sum_{i=1}^{p} [g_i(X)]^2 \tag{55}$$

$r = r_0^k$, $k$ is the number of iteration that must tend toward the infinity, and $r_0$ = 3. The problem will have $m$ additional unknown variables (Lagrange's multipliers $\lambda_i$) to be determined along with the engine's variables. The algorithm of the minimization process adopted here is the Broyden-Fletcher-Goldfarb-Shanno B.F.G.S. that sums up as follows:

1.  To start by an initial solution $X^{(0)}$.
2.  To estimate the solution at the k iteration by: $X_{k+1} = X_k - \alpha_k \cdot D_k \cdot \nabla f(X_k)$, with $X$ is a vector regrouping the optimization variables, $a_k$ is a relaxation factor, $\{D_k \cdot \nabla f(X_k)\}$ represents the decreasing direction of the function, $D_k^{-1}$ is an approximation of the Hessian matrix.
3.  To verify if the gradient's module of the objective function at the new vector X is under a certain desired value ($\approx 10^{-2}$). If it is true then this solution is the optimal solution, end of search. Otherwise increment k and return to the stage 2.

### 4.3.5 Results and discussion

We applied the optimization process explained in the previous section to two different profiles of inputs variables (fuel mass flow rate and resistant torque). The time step of discretization $h$ is equal to 0.01s and the time interval is equal to 3 sec, each problem has 900 unknown variables $\{w, P_a \text{ and } \dot{m}_c\}$ with 598 equalities constraints and 1800 inequalities constraints. Fig. 8 and 9 show a comparison between the results of the optimization process and the simulation's results of the engine's complete system model for the same input values and at fixed position of the turbine variable geometry (completely open, $GV$ = 0). The optimization's results show that we need significantly more air mass flow rate entering the intake manifold and higher intake pressure to reduce the opacity, while the real turbocharged diesel engine is not capable of fulfilling these tasks.
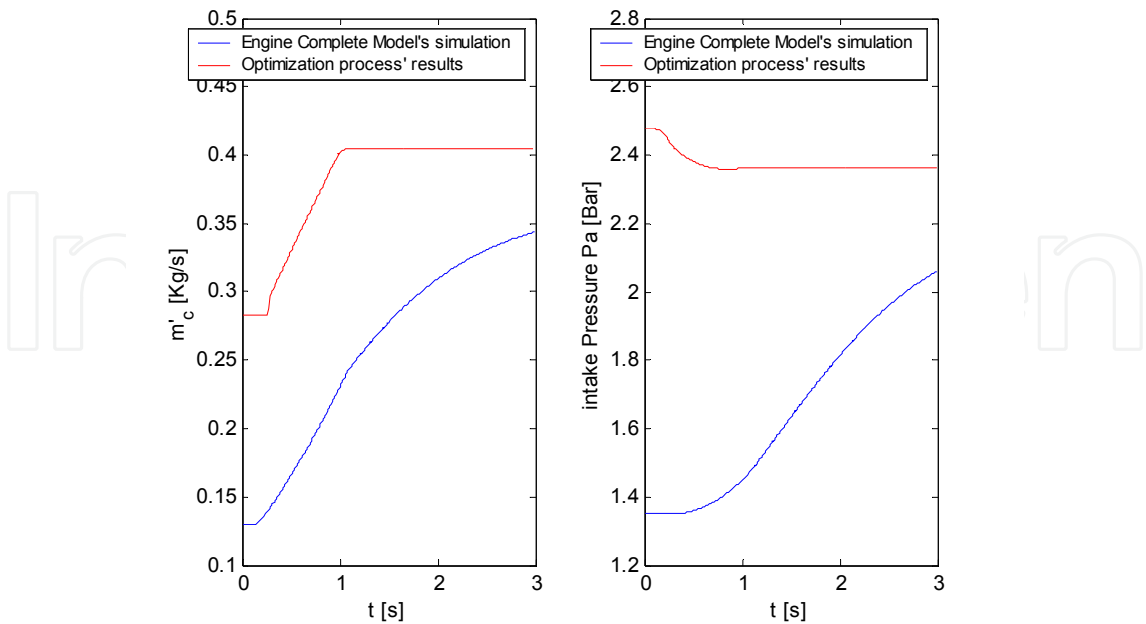


Fig. 8. Comparison between the air mass flow rate and the intake pressure calculated using the optimization procedure and the ones simulated using the engine complete model for a variable fuel flow rate and a constant resistant torque equal to 1000 N.m.
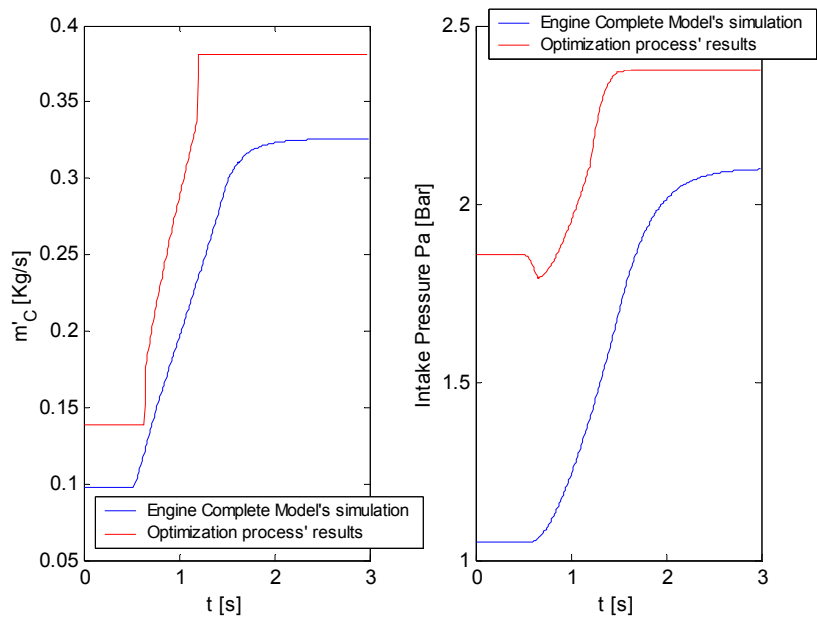
Fig. 9. Comparison between the air mass flow rate and the intake pressure calculated using the optimization procedure and the ones simulated using the engine's complete model for a variable fuel flow rate and a variable resistant torque.

Fig. 10 and 11 show a comparison between the simulated opacity derived from the optimization process and the one derived from the engine's complete system model for the same inputs used in fig. 8 and 9. The enormous gain in the opacity reduction proves the validity of the suggested optimization procedure.



Fig. 10. Opacity reduction using the optimal values of the air mass flow rate and the intake pressure. Blue: simulation without optimization, red: Simulation with optimization.

Fig. 11. Opacity reduction using the optimal values of the air mass flow rate and the intake pressure. Blue: simulation without optimization, red: Simulation with optimization.

## 4.4 Neural network controller

Optimization previously done "off line", would be directly unexploited "on-line" by a controlling processor seen the enormous computation time that is necessary to resolve the optimization problem. In order to integrate the results of this optimization's procedure in a closed loop controller (ref fig. 3), and to be able to use it in real time engine applications, we suggest to use a black box model based on neurons. Neural network is a powerful tool capable of simulating the engine's optimal control variables with good precision and almost instantly.

The neural network inputs are the fuel mass flow rate and the resistant torque, and its output variables are the optimal values of the air mass flow rate and the intake pressure. However in real time engine applications, the injected fuel flow rate is measurable, while the resistant torque is not. Consequently, we suggest substituting this variable by the crankshaft angular speed which can be easily measured and which is widely used in passenger cars controlling systems.

Firstly, we need to create a large database which will be used to train the neural model, and which covers all the functioning area of the engine in order to have a good precision and a highly engine performance. The database is created using the optimization process as explained in subsection 4.3.

Then we have to judicially choose the number of the inputs time sequence to be used, in order to capture the inputs dynamic effects and accurately predict the output variables. With intensive simulations and by trial and error, we find out that a neural network with inputs the fuel mass flow rate and the crankshaft angular speed at instant *(i)*, *(i-1)* and *(i-2)* is capable of precisely predicting the optimal values of the air mass flow rate and the intake

pressure at current instant *(i)*. Fig. 12 describes the neural network. The network is built using one hidden layer and one output layer, the activation functions of the hidden layer are sigmoid; the ones at the output layer are linear.
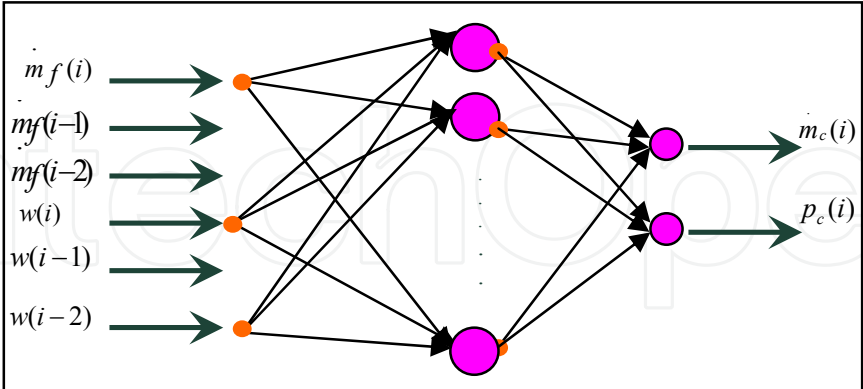


Fig. 12. The structural design of the neural network adopted in this paper for predicting the optimal control of the in-air filling and the intake pressure in real time applications.

The number of neurons in the hidden layer is determined by referring to the errors percentage of the points which are under a certain reference value wisely chosen; the errors percentage (table 3) are the results of the difference between the outputs of the network after the training process is completed, and the desired values used in the training database.

Table 3 shows the results of the neural networks with different number of neurons in their hidden layer, these networks are trained with the same database until a mean relative error equal to $10^{-8}$ is reached or maximum training time is consumed. The values in the table represent the percentage of the neural network results respecting the specified error percentage computed with respect to the reference values.

| Number of neurons of the hidden layer | Error percentage | | | Relative error |
|---|---|---|---|---|
| | < 1 % | < 5 % | < 10 % | |
| 110 | 57.71 | 88.85 | 96.71 | $3.6\ 10^{-5}$ |
| 120 | 98.428 | 100 | 100 | $10^{-8}$ |
| 130 | 98.734 | 100 | 100 | $10^{-8}$ |
| 140 | 99 | 100 | 100 | $10^{-8}$ |

Table 3. Results of four neural networks trained using different neurons number in their hidden layer and the same database.

The neural network adopted in this paper includes one hidden layer with 140 neurons and one output layer with 2 neurons. Fig. 13 and 14 show a comparison between the air mass flow rate and the intake pressure calculated using the theoretical optimization procedure, and the ones computed using the neural network. The results are almost identical; the mean relative error is $10^{-6}$.
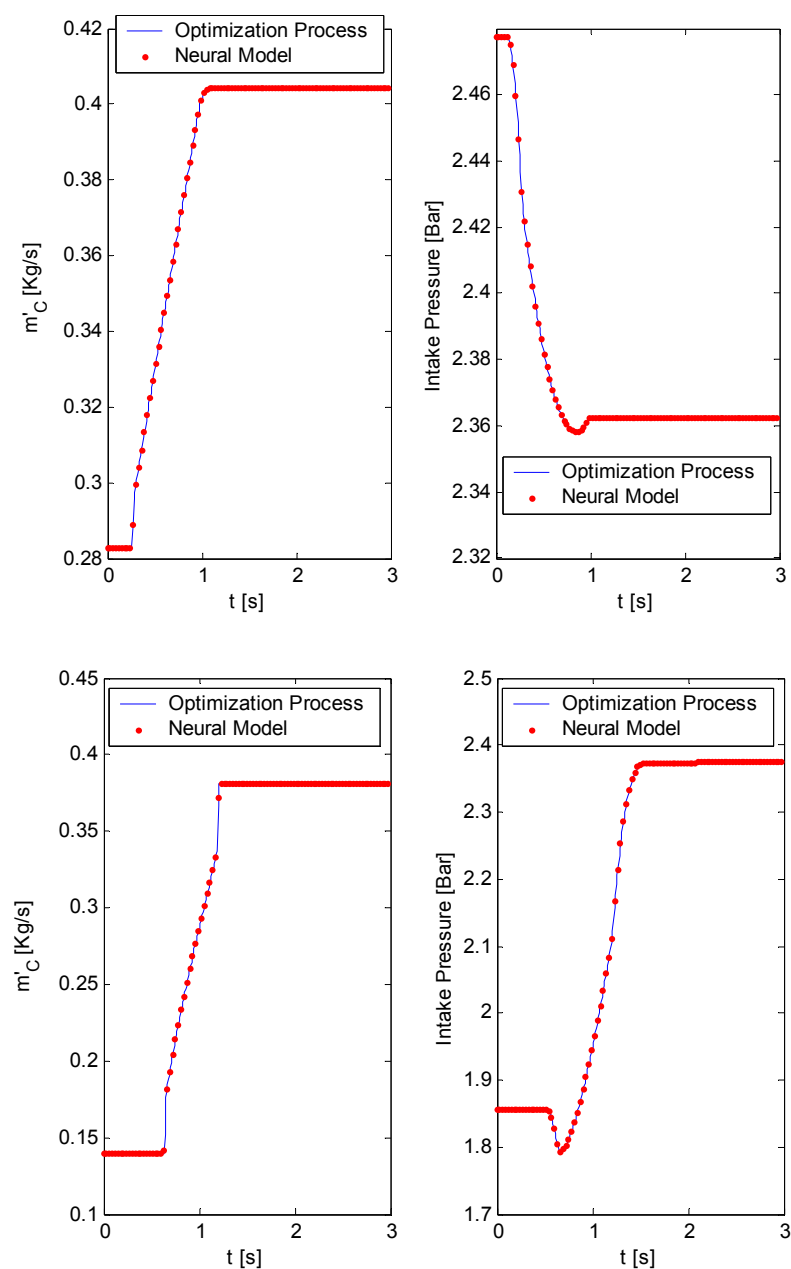
Fig. 13. & 14. Comparison between the neural network outputs and the optimal values of the air mass flow rate and the intake pressure.

## 5. General conclusions

We successfully developed and validated a mean value physical model that describes the gas states evolution and the opacity of a diesel engine with a variable geometry turbocharger. Then we proposed a dynamic control based on the optimal "in-air cylinders filling" in order to minimize the pollutants emissions while enhancing the engine performance. The optimization process is described in detail and the simulation results (fig. 8-11) prove to be very promising. In addition, the control principle as described here with the opacity criterion can be easily applied to other pollutants which have available physical model. This will be the object of future publications.

Also, in order to overcome on line computation difficulties, a real time dynamic control based on the neural network is suggested; therefore the optimal static maps of the fig. 2 can be successfully replaced by dynamic maps simulated in real time engine functioning (fig. 15).
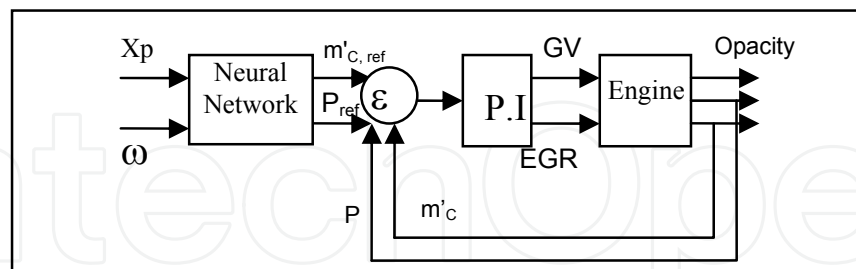


Fig. 15. Proposed control in closed loop

Finally, we should note that, in this chapter, while we did find, in theory, the optimal air mass flow rate and intake pressure necessary to minimize the opacity, but we didn't discuss the mechanical equipments required to provide the optimal intake pressure and intake air flow rate in real time engine applications. The practical implementation of the dynamic control is an important question to be studied thereafter. The use of a turbo-compressor with variable geometry and/or with Waste-Gate, and/or electric compressor is to be considered.

## 6. References

Arnold, J.F. (2007). *Proposition d'une stratégie de commande à base de logique floue pour la commande du circuit d'air d'un moteur Diesel.* PHD thesis, Rouen University, (March 2007), France.

Bai, L. & Yang, M. (2002). Coordinated control of EGR and VNT in turbocharged Diesel engine based on intake air mass observer, *SAE Technical paper* 2002-01-1292, (March 2002).

Bartoloni, G. (1989). Chattering Phenomena in Discontinuous Control Systems. *International Journal on Systems Sciences*, Vol. 20, Issue 12, (February 1989), ISSN 0020-7721.

Bellman, R. (1975). *Dynamic programming.* Princeton University Press, (1957), Princeton, NJ.

Doyle, J.C. (1979). Robustness of multiloop linear feedback systems" *Proceedings of the 1978 IEEE Conference on Decision and Control*, pages 12–18, Orlando, December 1979.

Dreyfus, S.E. (1962). Variational Problems with Inequality Constraints. *Journal of Mathematical Analysis and Applications*, Vol. 4, Issue 2, (July 1962), ISSN 0022-247X.

Friedland, B. (1996). *Advanced Control System Design.* Prentice-Hall, Englewood Cliffs, ISBN 978-0130140104, NJ, 1996.

Hafner, M. (2000). A Neuro-Fuzzy Based Method for the Design of Combustion Engine Dynamometer Experiments. *SAE Technical Paper* 2000-01-1262, (March 2000).

Hafner, M. (2001). Model based determination of dynamic engine control function parameters. *SAE Technical Paper* 2001-01-1981, (May 2001).

Hahn, W. (1967). *Stability of Motion*, Springer-Verlag, ISBN 978-3540038290, New York, 1967.

Hassenfolder, M. & Gissinger, G.L. (1993). Graphical eider for modelling with bound graphs in processes ». *ICBGM'93*, pp. 188-192, Californie, January 1993.

Jung, M. (2003). *Mean value modelling and robust control of the airpath of a turbocharged diesel engine.* Thesis for doctor of philosophy, University of Cambridge, 2003.

Kao, M. & Moskwa, J.J. (1995). Turbocharger Diesel engine modelling for non linear engine control and state estimation. *Trans ASME, Journal of Dynamic Systems Measurement and Control*, Vol. 117, Issue 1, pp. 20-30, (March 1995), ISSN 0022-0434.

Li, D.; Lu, D.; Kong X. & Wu G. (2005). Implicit curves and surfaces based on BP neural network. *Journal of Information & Computational Science*, Vol. 2, No 2, pp. 259-271, (2005), ISSN 1746-7659.

Minoux, M. (1983). *Programmation Mathématique, Théorie et Algorithmes. tome 1 & 2*, editions dunod, ISBN 978-2743010003, Paris 1983.

Omran, R.; Younes, R. & Champoussin, J.C. (2008a). Optimization of the In-Air Cylinders Filling for Emissions Reduction in Diesel engines, *SAE Technical Paper* 2008-01-1732, (June 2008).

Omran, R. ; Younes, R. & Champoussin, J.C. (2008b). Neural Networks for Real Time non linear Control of a Variable Geometry Turbocharged Diesel Engine, *International Journal of Robust and non Linear Control*, Vol. 18, Issue 12, pp. 1209-1229, (August 2008), ISSN 1099-1239.

Ouenou-Gamo, S. (2001). *Modélisation d'un moteur Diesel suralimenté*, PHD Thesis, Picardie Jules Vernes University, (2001), France.

Ouladssine, M.; Blosh, G. & Dovifazz X. (2004). Neural Modeling and Control of a Diesel Engine with Pollution Constraints. *Journal of Intelligent and Robotic Systems; Theory and Application*, Vol. 41, Issue 2-3, (January 2005), ISSN 0921-0296.

Outbib, R. & Vivalda, J.C. (1999). A note on Feedback stabilization of smooth nonlinear systems. *IEEE Transactions on Automatic Control*. Vol. 44, No 1, pp. 200-203, (August 1999), ISSN 0018-9286.

Outbib, R. & Richard, E. (2000). State Feedback Stabilization of an Electropneumatic System. *ASME Journal of Dynamic Systems Measurement and Control*. Vol. 122, pp 410-415, (September 2000), ISSN 0022-0434.

Outbib, R. & Zasadzinski, M. (2009). Sliding Modes Control, In: *Control Methods for Electrical Machines,* René Husson Editor, Ch. 6, pp. 169-204, 2009. Wiley, ISBN 978-1-84821-093-6, USA.

Pontryagin, L.S.; Boltyanskii, V.; Gamkrelidze, R.V & Mishchenko, E.F. (1962). *The Mathematical Theory of Optimal Processes*. 1962, John Wiley & Sons, USA

Rivals, I. (1995). *Modélisation et commande de processus par réseaux de neurones ; application au pilotage d'un véhicule autonome*, PHD Thesis, Paris 6 University, (1995), France.

Sira-Ramirez, H. (1987). Differential Geometric Methods in Variable-Structure Control. *International Journal of Control*, Vol. 48, Issue 2, (March 1987), pp. 1359-1390, ISSN 0020-7179.

Slotine, J-J.E. (1984). Sliding Controller Design for Non-linear System. *International Journal of Control*, Vol. 40, Issue 2, pp. 421-434, (March 1984), ISSN 0020-7179.

Utkin, V.I. (1992). *Sliding Modes in Control and Optimization*, Springer-Verlag, ISBN 978-0387535166, Berlin 1992.

Winterbonne, D.E. & Horlock, J.H. (1984). *The thermodynamics and gas dynamics internal combustion engines*. Oxford Science Publication, ISBN 978-0198562122, London 1984.

Younes, R. (1993). *Elaboration d'un modèle de connaissance du moteur diesel avec turbocompresseur à géométrie variable en vue de l'optimisation de ses émissions*. PHD Thesis, Ecole Centrale de Lyon, (November 1993), France.

Zames, G. (1981). Feedback and optimal sensitivity: Model reference transformations, multiplicative seminorms, and approximative inverse" *IEEE Transcations on Automatic Control*, Vol. 26, Issue 2, pp. 301–320, (June 1981), ISSN 0018-9286.

Zweiri Y.H. (2006). Diesel engine indicated torque estimation based on artificial neural networks. *International Journal of Intelligent Technology*, Vol. 1, No 1, pp. 233-239, (July 2006), ISSN 1305-6417.

**Applications of Nonlinear Control**

Edited by Dr. Meral Altınay

A trend of inverstigation of Nonlinear Control Systems has been present over the last few decades. As a result the methods for its analysis and design have improved rapidly. This book includes nonlinear design topics such as Feedback Linearization, Lyapunov Based Control, Adaptive Control, Optimal Control and Robust Control. All chapters discuss different applications that are basically independent of each other. The book will provide the reader with information on modern control techniques and results which cover a very wide application area. Each chapter attempts to demonstrate how one would apply these techniques to real-world systems through both simulations and experimental settings.

**How to reference**

In order to correctly reference this scholarly work, feel free to copy and paste the following:

# INTECH
open science | open minds